Mon. Not. R. Astron. Soc. **000**, 1–?? (2008) Printed 4 November 2008 (MN LATEX style file v2.2)

Planetpol polarimetry of the exoplanet systems 55 Cnc and τ Boo

⋆ P. W. Lucas[1] †, J. H. Hough[1], J. A. Bailey[2], M. Tamura[3], E. Hirst[1], D. Harrison[1]
[1] *Centre for Astrophysics Research, University of Hertfordshire, College Lane, Hatfield AL10 9AB, United Kingdom*
[2] *School of Physics, University of New South Wales, NSW 2052, Australia*
[3] *National Astronomical Observatory, Osawa 2-21-2, Mitaka, Tokyo 181, Japan*

Accepted 2008. Received 2008; in original form July 2008

ABSTRACT

We present very sensitive polarimetry of 55 Cnc and τ Boo in an attempt to detect the partially polarised reflected light from the planets orbiting these two stars. 55 Cnc is orbited by a hot Neptune planet (55 Cnc e) at 0.038 AU, a hot Jupiter planet (55 Cnc b) at 0.11 AU, and at least 3 more distant planets. The polarisation of this system is very stable, showing no sign of the periodic variations that would be expected if a short period planet were detected. The measured standard deviation of the nightly averaged Stokes Q/I and U/I parameters is 2.2×10^{-6}. We derive upper limits on the geometric albedo, A_G and planetary radius using Monte Carlo multiple scattering simulations of a simple model atmosphere. We assume Rayleigh-like scattering and polarisation behaviour (scaled by the maximum polarisation, p_m at 90°) and pressure insensitive extinction. Atmospheres in which multiple scattering plays only a small role have an almost linear relation between polarisation and A_G. In this case, the 4σ upper limit is $A_G < 0.13(R/1.2R_{Jup})^{-2}p_m^{-1}$ for 55 Cnc e. This is most easily explained if 55 Cnc e is relatively small, like GJ436b, and therefore not a pure H-He planet. The data do not provide a useful upper limit for 55 Cnc b. τ Boo is orbited by an unusually massive hot Jupiter planet. The data show a standard deviation in the night to night average Stokes Q/I and U/I polarisation parameters of 5.1×10^{-6}. The 4σ upper limit is $A_G < 0.37(R/1.2R_{Jup})^{-2}p_m^{-1}$ for τ Boo b, adopting the fairly well established orbital inclination $i\sim40°$. This extends the similar upper limits reported previously for this planet to longer wavelengths. The fact that the τ Boo data show more scatter, despite the smaller photon noise for this bright star, may be due to the spot activity detected photometrically by the *MOST* satellite. These results contrast markedly with the recent claim of a 3σ detection of a periodic polarisation signal from HD189733 with amplitude P= 2×10^{-4}, attributed to the planet HD189733 b.

Key words: (stars:) planetary systems – polarization – instrumentation: polarimeters – (ISM:) dust, extinction

1 INTRODUCTION

Since the seminal discovery of 51 Peg b (Mayor & Queloz 1995), ∼300 extrasolar planets have been found (e.g. Butler et al.2006, Schneider 2008). Approximately one third of these orbit very close to their central star, with semi-major axes, $a < 0.1$ AU (Schneider 2008). The number of short period planets is increasing rapidly with the growing success of transit based searches such as SuperWASP (Pollacco et al.2006) and HATNet (Bakos et al.2004), which are even more strongly biased towards such detections than the radial velocity method.

These close in planets offer the best opportunity to study the physical characteristics of the planets, as opposed to their orbital parameters. The combination of transit data and radial velocity data yields a precise planetary mass, size and density. Furthermore, recent studies with the *Spitzer* Space Telescope (e.g. Knutson et al.2007; 2008; Burrows et al.2007; Tinetti et al.2007) and the *Hubble* Space Telescope (e.g. Pont et al.2008; Swain et al.2008; Lecavelier

⋆ Based on observations made with the William Herschel Telescope operated on the island of La Palma by the Isaac Newton Group in the Spanish Observatory del Roque de los Muchachos of the Instituto de Astrofisica de Canarias.

† E-mail: P.W.Lucas@herts.ac.uk.

des Etangs 2008) have obtained a great deal of information about the chemical composition and pressure temperature profiles of the atmospheres of the two brightest transiting "hot Jupiter" planets, HD189733 b and HD209458 b. These studies used infrared photometry and spectroscopy of radiation emitted by the planets and optical spectrophotometry of the transit. All required exceptionally high signal to noise data for the integrated light of the star and planet. These results build on the more limited data provided by earlier space based studies, e.g. Charbonneau et al.(2002); Harrington et al.(2006).

While space-based observations have now produced high quality data on the atmospheres of these two planets, ground based observations have yet to produce a confirmed direct detection of an extrasolar planet. Neither space based nor ground based efforts have yet detected an extrasolar planet in reflected light. The MOST satellite has provided strong upper limits on the reflected light from HD209458 b (Rowe et al.2007) and ground based searches have also produced meaningful upper limits for a few planets (e.g. Charbonneau et al.1999; Leigh et al.2003; Winn et al.2008; Snellen 2005; Snellen & Covino 2007). Recently, Berdyugina et al.(2008) have reported a possible detection of reflected light from HD189733 b at low signal to noise, using ground based polarimetry with a conventional instrument employing slow modulation. However, the reported fractional polarisation is so large ($P \sim 2 \times 10^{-4}$) that it exceeds that expected for a perfectly reflective planet (i.e. a Lambert sphere with Rayleigh scattering polarisation properties) with the size indicated by the transit data, see Seager, Whitney & Sasselov (2000).

Polarimetry is nonetheless a promising method to detect extrasolar planets in reflected light. The basic principle is that reflected light is partially polarised (Seager et al.2000; Stam, Hovenier & Waters 2004; Stam et al.2006; Stam 2008) whereas the direct light emitted by stellar photospheres has negligible linear polarisation. Kemp et al.(1987) measured an upper limit on the integrated linear polarisation from the solar disc of $P < 2 \times 10^{-7}$ in the V band. Polarimetry therefore circumvents the contrast problem associated with extrasolar planets and their central stars. It can be used to detect planets that are spatially unresolved from the central star by searching for changes in the polarisation that have the same period as the planet's orbit (Seager et al.2000). In this case the time varying polarisation due to the planet will usually be superimposed on a constant polarisation that is caused by dichroic extinction in the interstellar medium along the line of sight to Earth. The interstellar polarisation of stars in the local ionised bubble within ∼100 pc of the sun is very small (typically P∼10^{-5}-10^{-6}, see Hough et al.2006) and is assumed to be constant during the period of an observing run, see §4.4. Alternatively, polarimetry can be used to assist in detecting planets that are spatially resolved from the central star by very high resolution imaging. This approach is be attempted with new instruments such as Hi-CIAO on Subaru, NICI and GPI on Gemini and SPHERE on the VLT.

In this paper we have adopted the first approach, using an aperture polarimeter to observe exoplanet systems in which the planet cannot be spatially resolved in the forseeable future. Hough et al.(2006) described the Planetpol instrument, which was specifically designed to achieve a sensitivity to fractional linear polarisations of order 10^{-6} by using a fast modulator system, similar in principle to that described by Kemp et al.(1987) and references therein. Polarimetry with fast modulators (which induce a rapid periodic variation of the relative retardance of electromagnetic vibrations in orthogonal planes) permits this very high sensitivity by separating the polarised component of the incident radiation field from the unpolarised component, converting the former into a high frequency signal in the time domain. This means that very small fractional polarisations can be measured without the need for very precise flux measurements with the detector. Planetpol achieves photon noise limited performance for bright exoplanet systems so the main limitation on the polarisation sensitivity is the need to gather in excess of 10^{12} photons in order to measure fractional polarisations as low as 10^{-6}. The fast modulation is performed by Photoelastic Modulators (PEMs) operated at 20 kHz, which is fast enough to remove any effects of the Earth's atmosphere.

By contrast, conventional polarimeters for night time astronomy employ slow modulation, rotating a waveplate with a fixed retardance of 0.5 wavelengths to several different position angles. Measurement of fractional polarisations of order 10^{-6} with such a system would require a precision of order 10^{-6} in the measured flux on the detector, which would be very challenging. In practice such polarimeters rarely achieve a sensitivity better than $P = 10^{-4}$.

While the recent space based measurements have revealed much about the atmospheres of two transiting planets the energy balance of these systems cannot yet be understood without measurement of their albedos. Most of the space based measurements have been obtained during transits, which only sample the upper layers of the atmosphere, not the principal reflecting layer. Even if space based spectroscopy is obtained outside transit events, it is difficult to infer the presence or absence of dust particles and their contribution to the radiative transfer without polarisation data. Successful polarimetric detection of exoplanets could address these questions and permit determination of the inclination of the planetary orbit (transiting systems are not required). For example, Hansen & Hovenier (1974) used ground-based aperture polarimetry to determine that sulphuric acid clouds, with ∼1 μm-sized droplets, dominate the reflection of sunlight from Venus.

Here we describe the results of Planetpol polarimetry of two exoplanet systems, 55 Cnc and τ Boo. The orbital parameters of their potentially detectable inner planets are listed in Table 1, taken from Butler et al.(2006) and Fischer et al.(2008) (with the exception of the inclinations, see below). These systems were selected on the basis that their bright I band magnitudes (brighter than any of the known transiting planets) and the short orbital period of their closest planetary companions made them good prospects to produce a detectable polarised flux.

The 55 Cnc system (HR3522) is a wide stellar binary, consisting of a G8IV-V primary (Baliunas et al.1997) with Cousins I mag=5.1 and an M4 secondary (Patience et al.2002; Eggenberger et al.2004; Raghavan et al.2006). The primary is now believed to be orbited by 5 planets (Fischer et al.2008; Butler et al.1997, Marcy et al.2002; McArthur et al.2004) and the inclination of the planetary orbits has some constraints from high precision astrometry of reflex motion

Table 1. Orbital parameters

Planet	$m.sin(i)$ (M_{Jup})	a (AU)	Period (d)	e	i
55 Cnc e	0.034	0.038	2.817	0.07±0.06	$\sim 55°$
55 Cnc b	0.824	0.115	14.652	0.014±0.008	$\sim 55°$
τ Boo b	4.13	0.0481	3.312	0.023±0.015	$\sim 40°$

caused by the outermost planet (McArthur et al.2004). It has an $R\prime_{HK}$ index of -4.97 (Soderblom 1985; Baliunas et al.1996) and a rotation period of 44 days (Soderblom 1985). The innermost planet, 55 Cnc e, is a "hot Neptune" and the next planet out, 55 Cnc b, is a hot Jupiter. Both planets could reasonably be expected to produce a detectable signal, although the relatively large orbit of 55 Cnc b (see Table 1) would require it to have a high albedo and a large radius, and the Neptune mass planet 55 Cnc e might also require a high albedo, depending on the size of the planet.

The τ Boo system (HR5185) is also a wide stellar binary composed of an F7IV-V primary (Baliunas et al.1997) with Cousins I mag=4.0 and an M2V secondary (Raghavan et al.2006). The primary is orbited by one of the most massive known hot Jupiter planets (Butler et al.1997), which is commonly referred to as τ Boo b. Baliunas et al.(1997; 1996) found the star to be photometrically stable at the millimagnitude level, with an $R\prime_{HK}$ index of -4.73. However, recent space based photometry by MOST has found that the stellar flux is variable at the millimagnitude level (Walker et al.2008). The period is consistent with the 3.3 day planetary orbit, suggesting that there is magnetic activity on the stellar surface that is linked to the planet. The changes in flux appear to be due mainly to a single star spot. However, the amplitude of the changes varies on long timescales, in some years apparently corresponding to a bright spot rather than a dark spot. τ Boo is believed to be a unique case where the massive planet has tidally spun up at least the outer layers of the star to have the same rotation period as the planet's orbit. The inclination of the stellar rotation axis can be determined from the measured photometric period and the $vsin(i)$ Doppler broadening of stellar lines as $i \approx 40°$, e.g. Leigh et al.(2003). Recent mapping of the magnetic field using (circular) spectropolarimetry (Catala et al.2007) also finds a similar intermediate inclination. Assuming that the planetary orbit shares this inclination, this allows the mass of the planet to be determined as $\sim$ 6-7 M_{Jup}.

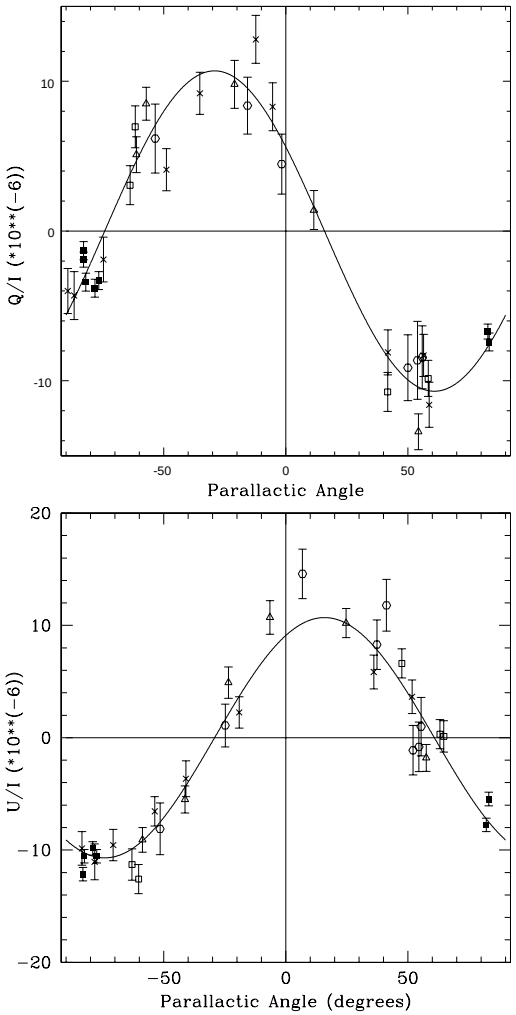

Figure 1. The fit to the telescope polarisation (TP) in the Februry 2006 observing run, plotted in instrumental coordinates. The data for the nearby bright stars that are used to construct the fit are plotted with different sysmbols for each star, after subtraction of the constant intrinsic Q/I and U/I values given in Table 2 (see Hough et al.2006 for a full explanation of the fitting procedure). The quality of the fit illustrates the polarisation stability of normal stars. Ten outlying measurements have been excluded from both the plot and the fit (see §2.3). *(upper panel)* Q/I; *(lower panel)* U/I. The error bars are the internal random errors on the measurements.

2 OBSERVATIONS

All observations were made with PLANETPOL mounted at the Cassegrain focus of the 4.2-m William Herschel Telescope at the Roque de los Muchachos Observatory on La Palma, one of the Canary Islands.

2.1 55 Cnc

55 Cnc was observed on 15-20 February 2006. The OG590 longpass filter was used in each case, leading to a central wavelength near 780 nm and a broad response between 590 and 920 nm. The long wavelength limit is determined by the response of the single element Avalanche Photodiode Detectors in PLANETPOL. The PEMs were set to an amplitude of 0.5 λ at 780 nm. The 55 Cnc system and the nearby low polarisation stars used to calibrate the telescope polarisation (TP) were all observed with a 5 arcsec diameter aperture. The observing procedure, system response and data reduc-

tion is described in Hough et al.(2006). The instrument simultaneously measures the total flux and the polarised flux within the aperture, providing Stokes I and Q data or Stokes I and U data, depending on the orientation of the instrument. The reduction script provides the corresponding Q/I or U/I value. The Stokes Q and U parameters are measured in the instrumental system and are later converted to the equatorial system. Integration times of 24 minutes on source were used for the individual Stokes Q and U data points for 55 Cnc. This time was split into 8 steps of 180 s each by the second stage chopping procedure, in which the orientation of the analyser and detector assemblies alternates between $+45^\circ$ and -45° relative to the PEMs, thereby reversing the sign of the measured polarisation in order to aid removal of systematic effects. With overheads for second stage chopping and readout the elapsed time for a Stokes Q or U data point was ≈ 28 minutes.

The nearby stars used to calibrate the TP were HR2421, HR2990, HR4534, HR4540 and HR4295. They were observed in the same manner as τ Boo, except that the time on source for individual Stokes Q and U measurements was 12 minutes, comprising only 4 steps. These stars all have low polarisation and are brighter than 55 Cnc, so this shorter integration time is sufficient to calibrate the TP with the requisite precision (Hough et al.2006). Their properties and mean fitted polarisations are summarised in Table 2. The individual measurements, after subtracting the fitted TP and the instrumental polarisation (IP), are listed in Table 3 to illustrate their stability. Note that the errors quoted in Table 3 are the internal random errors associated with each measurement. These typically underestimate the true errors slightly, see §2.3.

Planetpol has a separate optical channel which is used to measure the polarised flux from the night sky at a distance of ∼14 arcminutes from the target, in order to subtract this from the flux measured in the science channel. The February 2006 run occurred during bright time and for a significant fraction of the time there was a polarised flux from the sky (possibly enhanced by reflection of moonlight from very thin cirrus) that was of the same order as the polarised flux from 55 Cnc in the raw data. The stability of the subtracted measurements (see §3.1) indicates that this procedure worked well. There is much less photon noise in the sky measurements than in measurements of bright stars since it is a faint but highly polarised radiation field. Consequently the sky subtraction does not make a significant contribution to the total error budget.

The position angle and degree of polarisation were calibrated using the polarisation standards HD43384, HD154445, and HD21291 (Serkowski 1974)

2.2 τ Boo

τ Boo was observed in four observing runs on 24-26 April 2004, 25-30 April 2005, 7-8 May 2005 and 15-20 Feb 2006. The 2006 observing run was primarily devoted to 55 Cnc but a pair of Stokes Q/I and U/I observations of τ Boo were taken at the end of each night after 55 Cnc had set. The observing set up was as described above for 55 Cnc. The nearby bright stars used to calibrate the TP in the 2005 runs were HR5854, HR4534, HR4932 and HR 5435. Their physical characteristics and mean polarisations are given in Table 4 of Hough et al.(2006) and the individual measurements are listed in Table 2 of Bailey et al.(2008). In the 2004 run the stars used were HR4540, HR 5854 and HR5793. We do not list the individual measurements for these three stars, which were too few to carefully investigate their stability. However, the measurements are shown graphically in Figure 6 of Hough et al.(2006).

Data taken on 3-7 May 2005 were contaminated by a Saharan dust event above the observatory (Bailey et al.2008; Ulanowski et al.2007). This produced a polarisation of order 10^{-5} at large zenith distances which gradually declined throughout that period. We exclude the data taken on 3-6 May from our analysis but we include the τ Boo observations from 7 May, since this was at the end of the dust event and the observations were taken at zenith distances $\leqslant 20^\circ$, which reduced the effect on fractional polarisation to a level below the measurement error. The τ Boo data for that night are therefore useable but we have conservatively increased the uncertainty on the measurements by a factor of $\sqrt{2}$. Data from 7 May were not included in the calibration of TP. The data from the nights of 7 and 8 May provide useful repeat coverage of the same orbital phase as 27 and 28 April respectively (after an interval of 3 orbits).

The position angle and degree of polarisation was calibrated using the polarisation standards HD198478 and HD187929 in 2004. In April 2005 the standards HD187929, HD147084, HD198478 and HD154445 were used. In May 2005 the standards HD183143 and HD198478 were used. All were taken from Serkowski (1974).

2.3 Stability of Planetpol measurements

The random errors on measurements with Planetpol can be determined from the scatter of the residuals to TP fits, such as that shown in Figure 1. In Hough et al.(2006) we reported that these errors tended to be larger than the internal errors (determined from the standard deviation of the polarised flux within each measurement) by a factor of 1.6 to 1.8. In that work we reported that this factor did not show an obvious dependence on the flux from the star. However, the data on the five bright nearby stars in Table 3 include more repeat measurements of each star than previously, including the very bright star HR2990 (β Gem). This star has I mag=0.2, leading to a typical internal error on Q/I or U/I measurements of only 6×10^{-7}. The residuals to the TP fit for this star were more than three times this value on several occasions. Furthermore, some measurements of the other four bright stars deviated by $>3\sigma$ from the fit. Such measurements comprise 16% of the total (12/75) for these five stars. Ten of these outlying measurements deviated from the TP fit by $>3\times10^{-6}$ and were excluded from the fitting process. These discrepancies appear to be less common among the fainter stars, for which larger fractional errors in Q/I and U/I are expected, in proportion to photon noise. No 3σ errors were found for the faintest of the five stars, HR4540 (I mag=3.0), and the measurements of 55 Cnc (I mag=5.1) are all very stable and consistent with the expected scatter if no planet were detected, see §3.1.

It therefore seems likely that there is another source of error in addition to the random error due to photon noise (see §2.4). Inspection of the discrepant measurements showed that they are usually associated with disagreements

Table 2. Stars used to calibrate Telescope Polarisation during Feb 2006. Average polarisation measurements are given in the equatorial system.

Star	Spectral Type	Distance (pc)	I_c	V-I_c	Number of obs (Q/U)	<Q/I> ($\times 10^{-6}$)	<U/I> ($\times 10^{-6}$)
HR2421	A0IV	31.2	1.89	0.04	(5/6)	-1.49±1.21	-7.01±1.14
HR2990	K0III	10.3	0.19	0.97	(7/6)	-12.82±0.84	-12.04±0.92
HR4534	A3V	11.1	2.04	0.10	(4/5)	3.85±1.22	-6.01±1.28
HR4295	A1V	24.3	2.32	0.02	(10/8)	5.00±0.84	-8.19±0.99
HR4540	F8V	10.9	2.98	0.61	(6/8)	3.26±1.39	-0.12±1.14

Table 3. Individual Q/I and U/I measurements (in units of 10^{-6}) given in the instrumental system for the TP calibration stars used in Feb 2006.

Star	Date	Time	Q/I	σ	Date	Time	U/I	σ
HR2421	Feb 15	20:07	-6.5	1.3	Feb 15	20:25	2.0	1.2
HR2421	Feb 17	20:18	-4.2	1.2	Feb 17	21:08	0.7	1.3
HR2421	Feb 18	21:32	-7.4	1.7	Feb 18	21:46	5.3	1.6
HR2421	Feb 18	23:19	-10.2	1.3	Feb 18	23:34	-1.5	1.3
HR2421	Feb 19	22:01	-7.2	1.4	Feb 19	21:24	4.9	1.5
-	-	-	-	-	Feb 19	22:16	1.9	1.3
HR2990	Feb 15	21:56	-10.0	0.5	Feb 15	22:33	13.5	0.6
HR2990	Feb 16	00:14	-11.2	0.6	Feb 16	00:29	12.3	0.6
HR2990	Feb 16	19:54	-13.9	0.6	Feb 16	20:08	16.8	0.6
HR2990	Feb 16	21:53	-9.3	0.6	Feb 16	22:28	10.2	0.6
HR2990	Feb 17	21:28	-11.9	0.6	Feb 17	21:42	16.5	0.6
HR2990	Feb 18	00:36	-10.2	0.5	Feb 18	00:50	13.5	0.6
HR2990	Feb 20	20:00	-13.8	0.6	Feb 20	20:15	11.3	0.6
HR2990	Feb 21	03:25	-5.4	0.6	Feb 21	03:08	15.7	0.7
HR4534	Feb 16	00:49	-3.5	1.5	Feb 16	01:04	-5.7	1.4
HR4534	Feb 16	05:24	-5.3	1.3	Feb 16	05:40	-1.3	1.4
HR4534	Feb 17	00:12	-7.0	1.4	Feb 17	00:27	-3.4	1.5
HR4534	Feb 17	05:57	2.0	1.3	Feb 17	06:12	1.3	1.4
HR4534	Feb 18	04:08	-8.8	1.4	Feb 18	04:22	-3.9	1.4
HR4534	Feb 19	06:46	2.0	1.9	Feb 20	06:44	-4.1	1.5
HR4295	Feb 16	03:47	-9.8	1.5	Feb 16	04:02	-3.9	1.7
HR4295	Feb 16	06:59	-6.9	1.6	Feb 17	01:04	-7.1	1.6
HR4295	Feb 17	00:49	-8.1	1.6	Feb 17	04:35	-2.9	1.4
HR4295	Feb 17	04:21	-13.0	1.5	Feb 17	06:28	-4.2	1.6
HR4295	Feb 17	06:43	-8.2	1.7	Feb 18	00:16	-4.2	1.6
HR4295	Feb 18	00:02	-6.0	1.5	Feb 18	05:30	-3.4	1.5
HR4295	Feb 19	23:46	-9.5	1.6	Feb 20	00:02	2.2	1.6
HR4295	Feb 20	02:24	-7.3	1.7	Feb 20	02:39	-11.7	1.6
HR4295	Feb 20	05:38	-10.3	1.6	Feb 20	05:53	-5.1	1.7
HR4295	Feb 21	02:35	-4.2	1.7	Feb 21	02:50	-6.1	1.5
HR4540	-	-	-	-	Feb 18	04:43	-2.7	2.4
HR4540	-	-	-	-	Feb 18	04:58	2.2	2.5
HR4540	Feb 19	00:05	-1.3	2.5	Feb 19	00:20	-3.9	2.5
HR4540	Feb 19	05:41	0.6	2.4	Feb 19	05:55	-7.9	2.4
HR4540	Feb 19	06:11	1.6	2.8	Feb 19	06:26	-4.4	2.8
HR4540	Feb 20	02:58	-2.1	2.2	Feb 20	03:16	1.6	2.4
HR4540	Feb 20	06:27	2.0	2.3	Feb 20	06:12	-6.7	2.4
HR4540	Feb 21	02:17	-1.6	2.1	Feb 21	02:02	-3.8	2.1

in the measurements in the two beams in the science channel. These occasional differences in the two beams emerging from the Wollaston prism were previously reported in Hough et al.(2006) but their origin is not understood. We found no correlation between the discrepancies and the flux in the sky channel. Since deviations from the TP fit as high as 7-8$\times 10^{-6}$ have occasionally been seen in bright stars we surmise that this additional source of error is non-Gaussian and has a broader distribution of values. We conclude that more than one measurement of a science target should be taken whenever possible in order to guard against erroneous data. Even when obviously outlying measurements are excluded, the additional error source appears to impose a limit on the

sensitivity of PLANETPOL at a level slightly below 1×10^{-6}, see Table 2.

3 RESULTS

3.1 55 Cnc

The polarisation measurements for 55 Cnc are shown in Table 4 and Figure 2 (in the equatorial system), as a function of the orbital angle (ϕ) of 55 Cnc e. The angle ϕ=180° corresponds to minimum illumination of the observed hemisphere of the planet. The TP and the IP have been subtracted from the measurements, leaving only the astronomical signal, which we refer to as the residual polarisation. The data from different nights are plotted with different symbols. Individual nights cover only a small range in orbital angle so they can be usefully averaged. We have used the standard formula P=$\sqrt{Q^2+U^2-\sigma^2}/I$), where any negative P^2 values are set to zero. In general the internal uncertainties are very similar for the Q and U data so we have simply taken an average of the two for the uncertainty in P. The uncertainties in TP and IP make a negligible contribution to the total uncertainty, σ, of approximately 4.3×10^{-6} on each measurement that is used in the above formula.

The data cover three separated sections of the orbit of 55 Cnc e, each with a width of $\sim 50°$. Since the orbital period is close to 3 days the observations on 18 to 20 February 2006 repeated and broadened the orbital phase coverage of the data taken on 15 to 17 February. Allowing for the uncertainties, the average Q/I, U/I and P values are constant, i.e. the values are similar in the three sections of the orbit and the data from the two orbits agree well. The average values of Q/I, U/I and P are $\approx$ 0.2, -4.1 and 4.9 respectively, in units of $\times10^{-6}$. These very small values indicate that there is very little interstellar polarisation toward this nearby system (d=13 pc). This is consistent with the results for the nearby stars given in Table 2 and Hough et al.(2006): interstellar polarisation (which is caused by dichroic extinction by aligned dust grains) is of order 10^{-6} to 10^{-5} for stars within $\sim$ 30 pc.

The polarised flux from the night sky was detectable and comparable to the polarised flux from the 55 Cnc system for approximately half of the measurements, when the moon was above the horizon and not far from full phase. However, the consistency of the measurements indicates that the sky polarisation was generally well measured and subtracted.

3.2 τ Boo

All the polarisation measurements for τ Boo are shown in Figure 3(a-c) and Table 5 (in the equatorial system) as a function of the orbital angle of τ Boo b, with TP and IP subtracted. Again ϕ=180° corresponds to minimum illumination of the observed hemisphere. Data taken on different nights during the 2004 and 2005 observing runs are shown with different symbols. The 2006 data comprise just one datum per night for six nights and are all shown as small filled circles. The error bars are based on the internal standard error of $\approx 2.5\times10^{-6}$ for each measurement, which is mostly due to photon noise. The much smaller uncertainties in TP and IP make very little contribution to the total

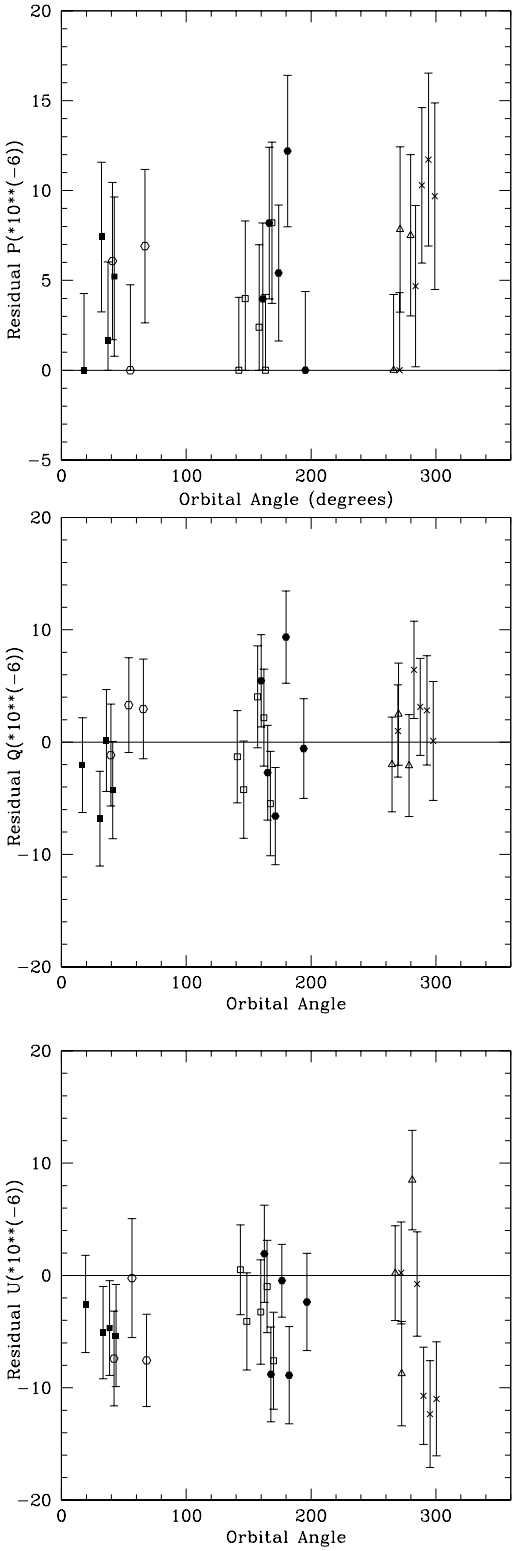

Figure 2. Polarisation of the 55 Cnc system as a function of the orbital angle, ϕ, of 55 Cnc e. Minimum illumination occurs at ϕ=180°. The polarisation of the telescope and the instrument have been subtracted. The data are plotted from ϕ=0 to 360°, as opposed to the usual -180 to 180°, in order to avoid splitting the data near 180°. *(top)* fractional polarisation (P=$\sqrt{Q^2+U^2-\sigma^2}/I$)); *(middle)* Q/I; *(bottom)* U/I. The data show no significant sign of variability within nights or between nights. Data points are assigned a different symbol for each of the six nights of observation.

errors. The average standard deviation of the τ Boo data within individual nights is only ≈16% higher than the internal standard error. This indicates that the plotted error bars are appropriate and there is no measurable variability in the polarisation of the τ Boo system on timescales of a few hours. It also tends to confirm our conclusion in §2.3 that photon noise usually dominates the error budget at this level of precision.

Overall, the data show somewhat more scatter than might be expected from the error bars, and certainly more than the data for 55 Cnc. We note that the Q/I and U/I data in Figures 3(b-c) are the measured independent quantities and that they should measure any changes in polarisation state more clearly than P. For example, the well sampled region between -165° and -115° includes data taken on 26 April 2004, 28 April 2005 and 8 May 2005. In units of 10^{-6} the average U/I values for these nights are -13.6 ± 3.0, 3.4 ± 3.2 and 7.6 ± 1.4 respectively (where the uncertainties are derived from the scatter in the measurements for each night). The first and last of these measurements differ from their mean value (-0.9×10^{-6}) by 4σ and 6σ respectively. The average Q/I measurements for these nights, in the same units, are 6.3±3.9, -2.2±1.4, -3.7 ±1.1 respectively. (For the latter two values the uncertainties are calculated from the internal photon-noise dominated uncertainties, since the scatter in the measurements happens to be smaller). The Q/I measurements lie closer to their mean, 0.1×10^{-6}, but the last measurement is 3σ below it.

The data taken in 2005 show less scatter than the full dataset. We plot the 2005 subset of the data separately in Figure 4(a-c). The standard deviations of the Q/I and U/I nightly averages for those nights in 2005 with more than one datum per night are 2.8×10^{-6} and 2.5×10^{-6} respectively. When we include all nights from 2004 and 2005 with more than one datum the standard deviations increase to 3.6×10^{-6} in Q/I and 6.5×10^{-6} in U/I. The large standard deviation in U/I is due in part to the two very negative readings at orbital angle, ϕ≈-160°, taken on 26 April 2004. However, the 2006 data also show a large standard deviation of 7.0×10^{-6} in U/I, so the large scatter seen in Figure 3(a-c) cannot be readily attributed to just one or two outlying readings.

Despite these signs of variability in the polarisation of τ Boo there is no sign of the peaks and troughs in Q/I or U/I predicted by the models shown in Figure 6(a-c) that would be most likely if reflected light from an extrasolar planet had been detected (see §4.2). The average values of $|Q/I|$ and $|U/I|$ are $< 10^{-6}$. These very small values indicate that there is very little interstellar polarisation toward this nearby star system (d=15pc). This is consistent with the result for 55 Cnc and the results for the nearby stars given in Table 2 and in Hough et al.(2006).

Quasi-periodic millimagnitude photometric variations in the optical light from τ Boo have been detected by the MOST microsatellite (Walker et al.2008). This was attributed to strong star spot activity. Reduced flux due a large spot was seen in 2004, located 65° in advance of the sub-planetary point. In 2005 the amplitude of the flux variations was much smaller and on one occasion the spot appeared bright rather than dark. They suggest that this is due to a magnetic interaction between the star and the planet, see also Shkolnik et al.(2005).

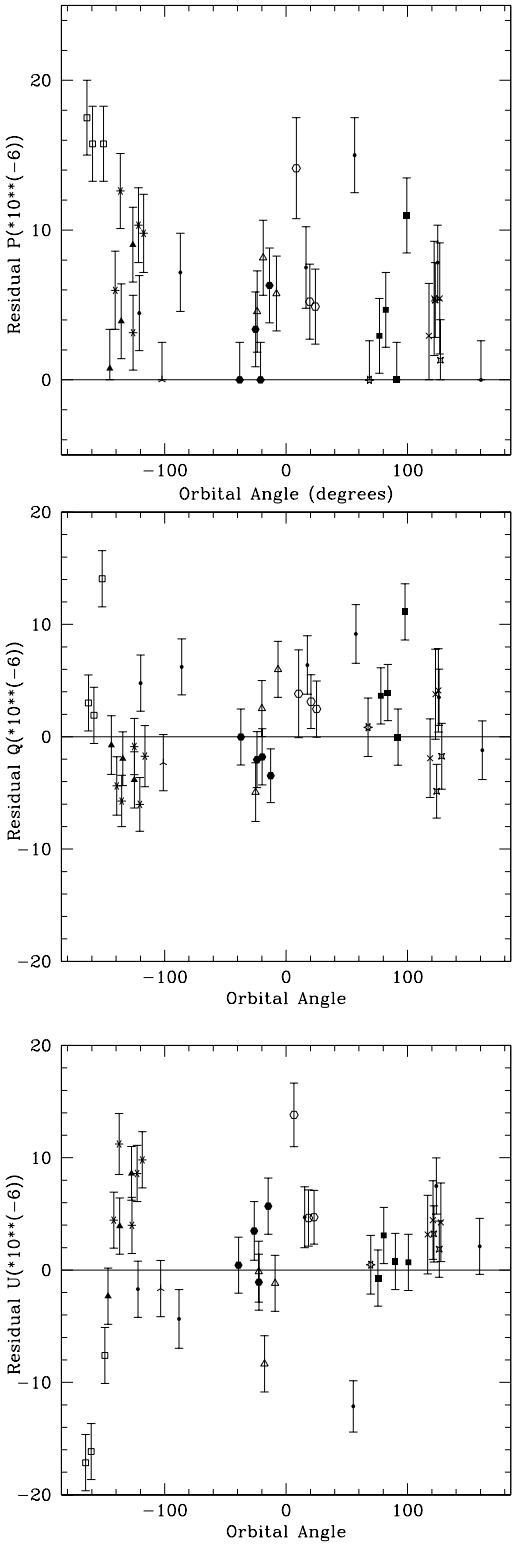

Figure 3. Polarisation of the τ Boo system as a function of the orbital angle of τ Boo b. The polarisation of the telescope and the instrument have been subtracted. *(top)* fractional polarisation, P; *(middle)* Q/I; *(bottom)* U/I. Data taken on each night have similar orbital angles. The 2004 and 2005 data have a unique symbol for each night. The 2006 observations had only 1 datum per night and are plotted with small filled circles. Overall, the observations show good agreement within each night but there is a somewhat larger scatter between nights than would be expected from a constant interstellar polarisation. There is no sign of periodic variability at the 3.3 day period of the planet.

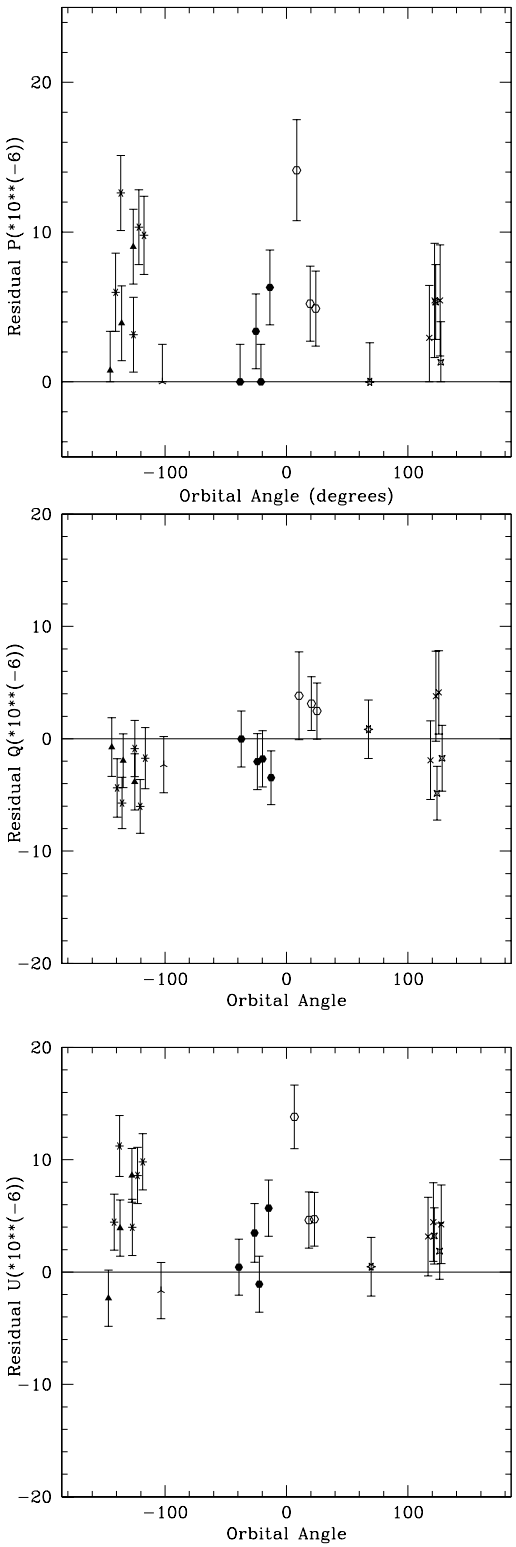

Figure 4. Polarisation of the τ Boo system in April-May 2005 as a function of the orbital angle of τ Boo b. The polarisation of the telescope and the instrument have been subtracted. *(top)* fractional polarisation, P; *(middle)* Q/I; *(bottom)* U/I. Data taken on each night have similar orbital angles. A different symbol is used for each night. These plots show less scatter than the plots of all the data in Figure 3.

The greater stability of our data in 2005 is consistent with the greater photometric stability in that year, if the polarisation variability is linked to star spots. Spot activity can induce weak linear polarisation in two ways. One way is through the transverse Zeeman effect (e.g. Kemp & Wolstencroft 1973; Borra & Vaughn 1976) but since that is a line effect and the global magnetic field of τ Boo is fairly weak (Catala et al.2007) this seems unlikely. The other possibility is that star spots are breaking the symmetry of the polarisation of the stellar disc. Stellar discs have a centrosymmetric polarisation pattern due to light scattering (Leroy 2000), with maximum polarisation very close to the limb of the star. In a uniform, spherically symmetric star the net polarisation will be zero but star spots near the limb can produce a measurable polarisation by breaking the symmetry, see Carciofi & Magalhaes (2005).

We might therefore expect to see low level polarisation with a 3.3 day period but with differences between our 2004 and 2005 measurements. While no periodic variations in polarisation are detected, the data were less stable in 2004 than 2005. However, the dataset is too small to permit us to distinguish variations on a timescale of days from variations between these two years. This issue clearly complicates any attempts to detect τ Boo b in polarised light.

Table 4. Individual measurements for 55 Cnc. Telescope Polarisation and Instrumental Polarisation have been subtracted. Orbital angle ϕ=180° corresponds to minimum illumination of the observed hemisphere.

Date	ϕ_Q	Q/I ($\times 10^{-6}$)	ϕ_U	U/I ($\times 10^{-6}$)	$<\phi>$	P
15/2/06	264.8	-2.0±4.2	267.4	0.2±4.2	266.1	$0.0^{+4.2}$
15/2/06	270.1	2.5±4.5	272.6	-8.7±4.6	271.4	7.8±4.6
15/2/06	278.5	-2.1±4.5	281.1	8.5±4.4	279.8	7.5±4.5
16/2/06	16.8	-2.0±4.2	19.3	-2.5±4.3	18.1	$0.0^{+4.3}$
16/2/06	30.8	-6.8±4.2	33.4	-5.1±4.1	32.1	7.4±4.2
16/2/06	36.0	0.1±4.5	38.6	-4.7±4.2	37.3	1.6±4.4
16/2/06	41.1	-4.3±4.3	43.7	-5.3±4.5	42.4	5.2±4.4
17/2/06	140.9	-1.3±4.1	143.4	0.5±4.0	142.2	$0.0^{+4.1}$
17/2/06	146.0	-4.2±4.3	148.5	-4.1±4.3	147.2	4.0±4.3
17/2/06	157.1	4.0±4.5	159.7	-3.2±4.6	158.4	2.4±4.6
17/2/06	162.2	2.2±4.3	164.8	-1.0±4.1	163.5	$0.0^{+4.2}$
17/2/06	167.4	-5.5±4.6	169.9	-7.6±4.3	168.7	8.2±4.5
18/2/06	269.6	1.0±4.1	272.2	0.2±4.5	270.9	$0.0^{+4.3}$
18/2/06	282.5	6.4±4.3	285.0	-0.8±4.6	283.8	4.7±4.5
18/2/06	287.5	3.1±4.3	290.1	-10.7±4.3	288.8	10.3±4.3
18/2/06	292.8	2.8±4.9	295.3	-12.3±4.8	294.1	11.7±4.8
18/2/06	297.9	0.1±5.3	300.5	-11.0±5.1	299.2	9.7±5.2
19/2/06	39.6	-1.2±4.5	42.1	-7.4±4.2	40.9	6.1±4.4
19/2/06	53.9	3.3±4.2	56.5	-0.2±5.3	55.2	$0.0^{+4.8}$
19/2/06	65.6	3.0±4.4	68.2	-7.6±4.1	66.9	6.9±4.2
20/2/06	160.0	5.5±4.1	162.6	1.9±4.3	161.3	4.0±4.2
20/2/06	165.2	-2.7±4.2	167.8	-8.8±4.2	166.5	8.2±4.2
20/2/06	171.4	-6.6±4.3	176.6	-0.5±3.2	174.0	5.4±3.8
20/2/06	179.9	9.4±4.1	182.4	-8.9±4.3	181.2	12.2±4.2
20/2/06	194.1	-0.6±4.4	196.7	-2.4±4.3	195.4	$0.0^{+4.4}$

Table 5. Individual measurements for τ Boo. Telescope Polarisation and Instrumental Polarisation have been subtracted. Orbital angle ϕ=180° corresponds to minimum illumination of the observed hemisphere.

Date	ϕ_Q	Q/I ($\times 10^{-6}$)	ϕ_U	U/I ($\times 10^{-6}$)	$< \phi >$	P
24/04/04	-22.47	-4.9 ±2.5	-25.17	-0.1 ±2.6	-23.82	4.6±2.7
24/04/04	-17.82	2.5 ±2.2	-20.0	-8.4 ±2.3	-18.91	8.2±2.5
24/04/04	-9.09	6.0 ±2.6	-6.71	-1.2 ±2.3	-7.9	5.8±2.5
25/04/04	75.69	3.6 ±2.5	77.99	-0.7 ±2.3	76.84	2.9±2.5
25/04/04	80.44	3.9 ±2.7	83.82	3.1 ±2.5	82.13	4.7±2.5
25/04/04	89.97	0.0 ±2.4	92.13	0.8 ±2.3	91.05	$0.0^{+2.5}$
25/04/04	100.7	11.1 ±2.4	97.96	0.7 ±2.3	99.35	11.0±2.5
26/04/04	-165.1	3.0 ±2.6	-162.8	-17.1 ±2.6	-163.9	17.5±2.5
26/04/04	-160.5	1.9 ±2.5	-158.2	-16.2 ±2.5	-159.4	15.8±2.5
26/04/04	-149.2	14.1 ±2.6	-151.5	-7.6 ±2.4	-150.4	15.8±2.5
25/04/05	-103.3	-2.3 ±2.5	-101.1	-1.6 ±2.5	-102.2	$0.0^{+2.5}$
26/04/05	6.5	3.8 ±3.9	10.3	13.8 ±2.8	8.4	14.1±3.4
26/04/05	18.5	3.1 ±2.4	20.5	4.6 ±2.5	19.5	5.2± 2.5
26/04/05	23.0	2.5 ±2.5	25.1	4.7 ±2.4	24.05	4.9±2.5
27/04/05	121.7	-4.9 ±2.4	124.0	3.2 ±2.5	122.8	5.3±2.5
27/04/05	126.1	-1.7 ±2.9	128.1	1.9 ±2.5	127.1	1.3±2.7
28/04/05	-146.6	-0.7 ±2.6	-143.9	-2.3 ±2.5	-145.2	0.8±2.6
28/04/05	-137.0	-2.0 ±2.4	-134.5	3.9 ±2.5	-135.8	3.9±2.5
28/04/05	-127.3	-3.8 ±2.5	-125.0	8.6 ±2.4	-126.1	9.0±2.5
29/04/05	-39.2	-0.0 ±2.5	-37.2	0.4 ±2.5	-38.2	$0.0^{+2.5}$
29/04/05	-26.3	-2.0 ±2.5	-24.0	3.5 ±2.6	-25.15	3.4±2.5
29/04/05	-22.4	-1.8 ±2.5	-19.7	-1.1 ±2.5	-21.05	0.0±2.5
29/04/05	-14.7	-3.5 ±2.4	-12.7	5.7 ±2.5	-13.7	6.3±2.5
30/04/05	69.7	0.8 ±2.6	67.5	0.5 ±2.6	68.6	$0.0^{+2.6}$
7/05/05	116.6	-1.9 ±3.5	118.6	3.2 ±3.5	117.6	2.9±3.5
7/05/05	120.9	3.8 ±4.0	123.0	4.5 ±3.5	121.9	5.4±3.8
7/05/05	127.5	4.1 ±3.7	125.4	4.3 ±3.5	126.4	5.4±3.7
8/05/05	-141.9	-4.4 ±2.6	-139.5	4.4 ±2.5	-140.7	6.0±2.6
8/05/05	-137.5	-5.7 ±2.3	-135.4	11.2 ±2.7	-136.4	12.6±2.5
8/05/05	-127.0	-0.9 ±2.5	-125.0	4.0 ±2.5	-126.0	3.2±2.5
8/05/05	-122.7	-6.0 ±2.4	-120.5	8.6 ±2.5	-121.6	10.3±2.5
8/05/05	-118.4	-1.7 ±2.7	-116.3	9.8 ±2.5	-117.4	9.8±2.6
16/02/06	55.3	9.1 ±2.6	57.5	-12.1±2.3	56.4	15.0±2.5
17/02/06	159.4	-1.2 ±2.6	161.6	2.1 ±2.5	160.5	$0.0^{+2.6}$
18/02/06	-88.2	6.2 ±2.5	-86.0	-4.3 ±2.6	-87.1	7.2±2.6
19/02/06	15.3	6.4 ±2.6	17.5	4.7 ±2.7	16.4	7.5±2.7
20/02/06	123.7	3.5 ±2.5	125.9	7.5 ±2.5	124.8	7.8±2.5
21/02/06	-122.0	4.8 ±2.5	-119.8	-1.7 ±2.5	-120.9	4.5±2.5

4 MODELLING AND DISCUSSION

4.1 Initial assumptions

We model the possible polarisation signatures of extrasolar planets with a Monte Carlo multiple scattering code with a radiative transfer similar to that used in Seager, Whitney & Sasselov (2000) and described in Green et al.(2003). The finite angular size of the star is included, with a solar limb darkening model (Claret 2000), and the eccentricity of the orbit is set to zero. All photons are assumed to hit the star-facing side of the planetary disc at randomly generated locations. Unlike Seager et al. we do not use a full model atmosphere with precisely specified composition and pressure-temperature profile. These quantities are hard to estimate and many of the variables will not affect the broad band polarised light signal of the planet. Instead we simply assume that the broad band radiative transfer will be dominated by Rayleigh scattering by molecules or Mie scattering by dust particles and we do not explicitly include molecular or atomic absorption. Our code assumes a uniform, locally plane parallel semi-infinite atmosphere with no variation of density with depth. In such a geometry, adding molecular or atomic absorption features would be equivalent to reducing the single scattering albedo.

In real atmospheres, molecular and atomic absorption features are pressure sensitive, whereas the single scattering albedo of dust particles is not, so their effects cannot simply be combined in a single parameter for each wavelength (see Prather (1974) and references therein). However, our assumption of a uniform atmosphere allows us to express in a simple manner the relation between the data and attributes of planets such as the geometric albedo and the radius.

For the individual scattering events, the models considered here have either exactly the Rayleigh scattering phase functions and Rayleigh angular dependence of polarisation or else are Rayleigh-like. The exact Rayleigh phase functions and polarisation behaviour is appropriate for either Rayleigh scattering by molecules or scattering by spherical dust particles (Mie scattering) that are much smaller than the wavelength of observation. This is because Mie scattering becomes identical to Rayleigh scattering in the limit of small particle size, except in one respect, which is that the albedo of very small dust particles will usually be less than unity. The *Rayleigh-like* models are Mie scattering models in which the size of the optically dominant particles is smaller than the wavelength but not small enough to be in the Rayleigh limit. In this size regime Mie scattering has a similar phase function to Rayleigh scattering but a higher probability to scatter photons forward rather than backward. The angular dependence of polarisation is also similar to Rayleigh scattering (a bell-shaped curve with maximum polarisation occuring at scattering angles near 90°) but the maximum polarisation is less than 100%.

In this regime, the most important model atmosphere parameters governing the polarised flux reflected from the planet are the single scattering albedo, ϖ and the maximum fractional polarisation produced by scattering of unpolarised light through 90°, p_m. As noted above, reducing ϖ is equivalent to introducing unspecified molecular absorption into the atmosphere. Models with larger dust grains produce a very different behaviour, generally with a lower polarised flux (see Seager et al.2000). However, such models are somewhat less probable because any large grains are predicted to settle below the photosphere under gravity (e.g. Helling, Woitke & Thi 2008; Ackerman & Marley 2001). The atmospheres of Jupiter and Saturn exhibit a combination of Rayleigh scattering and scattering by aerosols, some of which are small compared to the ∼0.78 μm wavelength of the filter employed here and some of which are larger, e.g. Leroy (2000) and references therein.

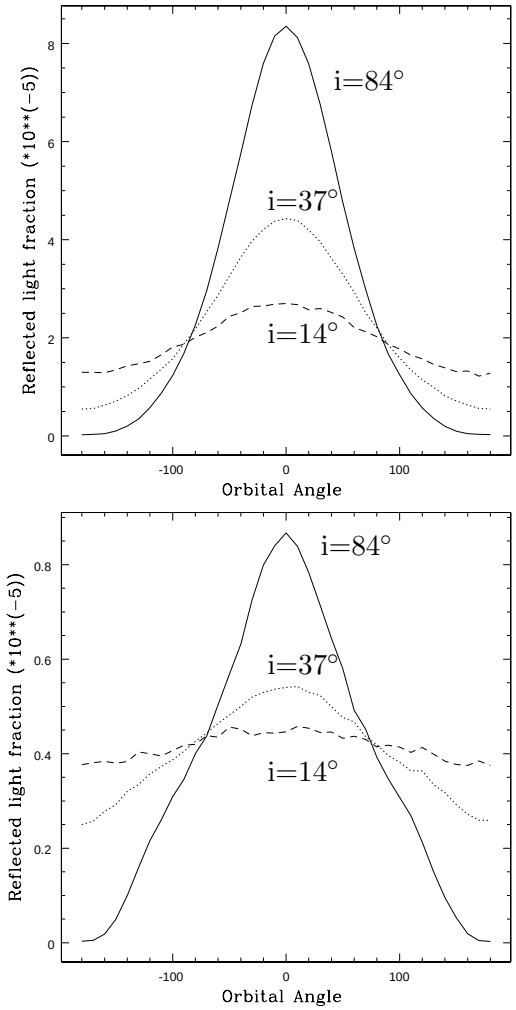

Figure 5. Reflected light curves. The reflected light from the planet is divided by the light from the star to give the fractional change in flux from the star+planet system. Solid lines: i=84°. Dotted lines: i=37°. Dashed lines: i=14°. *(upper panel)* "Rayleigh scattering" model, using ϖ=0.99. *(lower panel)* Interstellar dust (ISD) model. The ISD model produces an order of magnitude less reflected light due to weaker back scattering in the phase function and a lower single scattering albedo, see text §4.2. Note that the curves are not perfectly symmetric about ϕ=0 due to shot noise in the Monte Carlo simulations.

The orbital radius, r, is an additional parameter in our code. For very small orbital radii the incident radiation field becomes significantly non-parallel. However, we find that for the orbital radii of the planets considered in this paper ($r \geqslant 0.038$ AU) this makes a negligible difference to the results, by comparison with the plane parallel case for the same orbital radius. This extends the result of Seager et al.(2000), who also found this to be the case for the re-

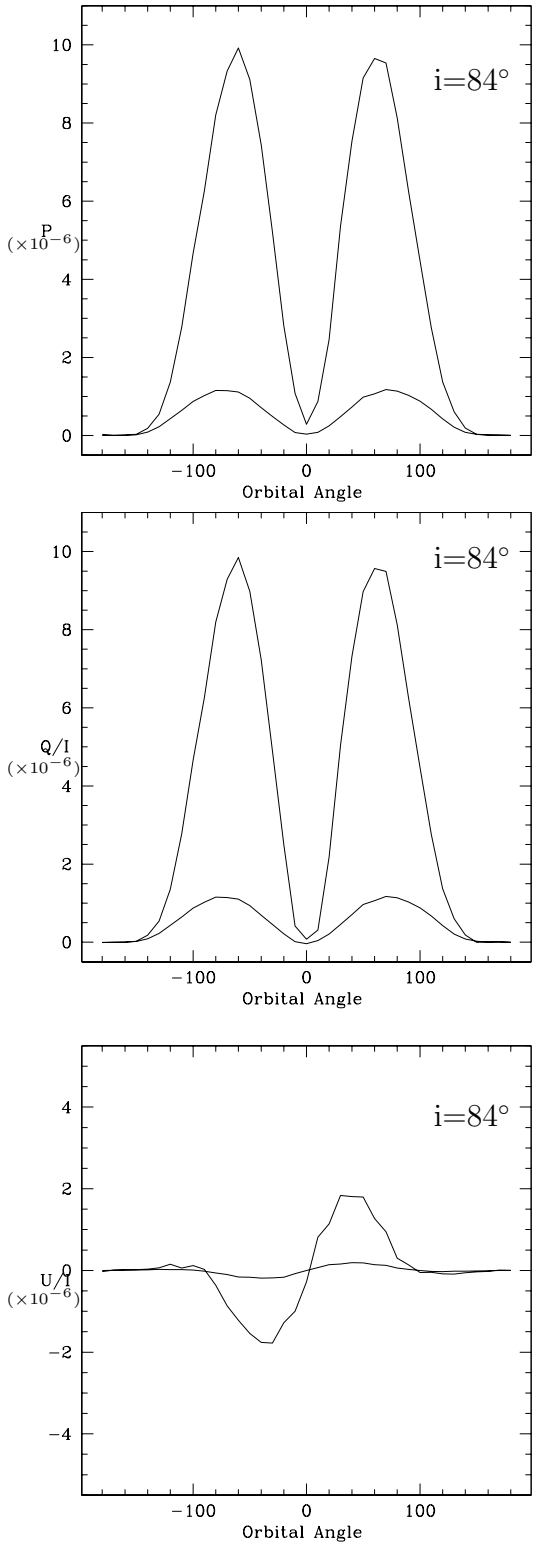

Figure 6. Model polarisation for orbital inclination $i = 84°$. *(top)* fractional polarisation, P; *(middle)* Q/I; *(bottom)* U/I. The curves with larger amplitude are for a Rayleigh scattering atmosphere. The curves with smaller amplitude are for an interstellar dust model (see text).

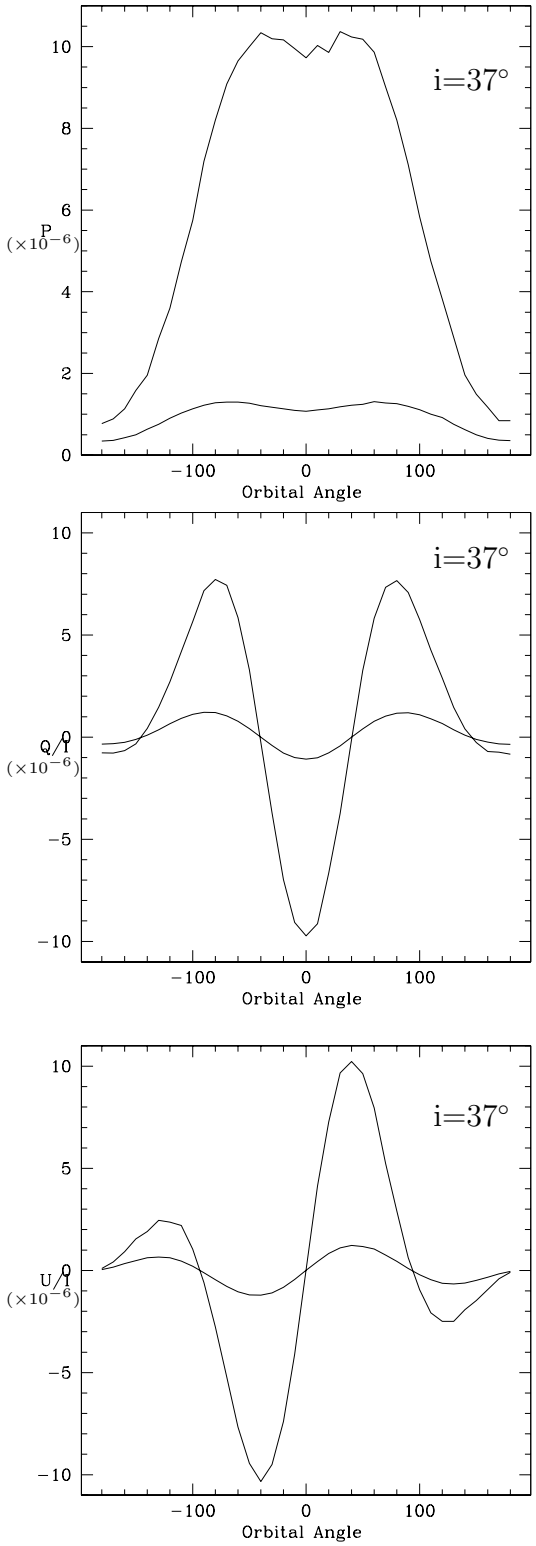

Figure 7. Model polarisation for orbital inclination $i = 37°$. *(top)* fractional polarisation, P; *(middle)* Q/I; *(bottom)* U/I. The curves with larger amplitude are for a Rayleigh scattering atmosphere. The curves with smaller amplitude are for an interstellar dust model (see text). Note that the plots of P and Q/I are not perfectly symmetric about ϕ=0 due to shot noise in the Monte Carlo simulations.

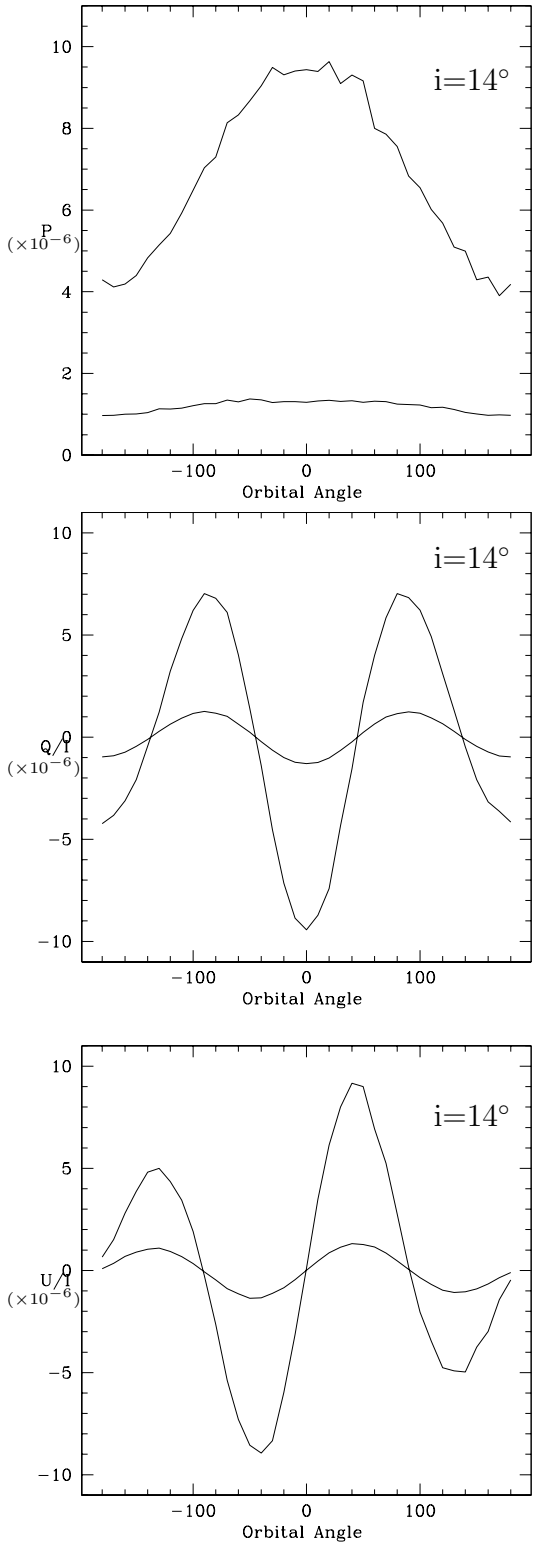

Figure 8. Model polarisation for orbital inclination $i = 14°$. *(top)* fractional polarisation, P; *(middle)* Q/I; *(bottom)* U/I. The curves with larger amplitude are for a Rayleigh scattering atmosphere. The curves with smaller amplitude are for an interstellar dust model (see text).

flected flux curves when dealing with reasonably isotropic phase functions but did not comment on the effect on the polarised light curves. However, Seager et al.(2000) and Green et al.(2003) found that a non-parallel radiation field does lead to significantly different reflected light curves for models that use highly forward throwing phase functions.

We have bench tested our code against the results of Prather (1974) and Stam et al.(2006). Prather (1974) calculated geometric albedo as a function of ϖ for a planet with a semi-infinite Rayleigh scattering atmosphere, assuming a plane parallel incident radiation field. Stam et al.(2006) used a locally analytical method combined with a numerical method for integrating over the planetary disc to calculate both polarisation and the reflected light curve for a planet with a pure Rayleigh scattering atmosphere (ϖ=1) and an optical depth of 5.75, with a black surface below. Again, a plane parallel incident radiation field was assumed. Our code accurately reproduces the polarisation curve shown in Figure 7 of Stam et al.(2006), including the polarisation reversal that occurs at small scattering angles (i.e. close to the "new moon" phase) due to multiple scattering effects. Our calculated geometric albedos agree with those of Prather (1974) to within 5%. In addition, our fractional polarisation curves for Rayleigh scattering models appear to be in good agreement with those shown in Seager et al.(2000) for atmospheres with 0.1 μm grains, although a precise quantitative comparison is not possible because of the much more complicated model atmospheres used in that work. The method of Stam et al.(2006) has the advantage that it can produce results with excellent precison for homogeneous atmospheres, whereas the Monte Carlo method has low signal to noise for calculations close to the new moon phase of a planet, owing to the small number of photons. However, our Monte Carlo approach has the advantages of (i) greater flexibility to treat vertically and horizontally inhomogeneous atmospheres and (ii) the ability to treat planets very close to the central star, where the incident radiation field is not plane parallel.

4.2 Sensitivity to planets

In Figures 5, 6, 7 and 8 we show the reflected light curves and the fractional P, Q/I and U/I outputs from two 20 million photon runs with different model atmospheres. Both simulations are for a planet with radius R=1.2 R_{Jup} (which is the typical size of a hot Jupiter) in a circular orbit at r=0.05 AU around a star with radius R_*=7×10^{8}m. In both cases the positive Stokes Q plane lies parallel to the axis of the orbit. Figure 6 shows the polarisation when the system has an orbital inclination $i = 84°$, Figure 7 shows it for $i = 37°$ and Figure 8 shows it for $i = 14°$. The upper panel of Figure 5 and the curves with larger amplitude in Figures 6-8 are for a run approximating a pure Rayleigh scattering atmosphere, the only difference being that the adopted single scattering albedo is ϖ=0.99 rather than unity, in order to ensure that the run completed in a finite time. The lower panel of Figure 5 and the curves with smaller amplitude in Figures 6-8 are for an atmosphere composed entirely of interstellar dust grains, using a silicate and graphite interstellar dust model taken from Fischer, Henning & Yorke (1994) in which the grains have sizes between 0.005 and 0.25 μm and an $n(r) \propto r^{-3.5}$ distribution within that range. This model

is run for a wavelength of 0.78 μm, at which ϖ=0.57 and p_m=0.4.

Figure 6(a) shows that maximum polarisation of the planetary system occurs near orbital angle ϕ=±60° (a gibbous phase) for orbital inclinations close to 90°. This is because the fractional polarisation of light reflected by the planet (which is greatest at ϕ=±90°) is modulated by the reflected light curves in Figure 5 when calculating the fractional polarisation of the star+planet system. The maximum polarised flux from the planet therefore occurs at a gibbous phase.

The models show that Rayleigh scattering and Mie scattering by small grains produce polarisation signals with a qualitatively similar dependence on orbital angle, ϕ. The maximum fractional polarisation, P, produced by the interstellar dust model is approximately a tenth of that produced by the Rayleigh scattering model. This is due to the combination of the smaller values of ϖ and p_m and weaker backscattering in the phase function. The interstellar dust mixture has a moderately forward throwing phase function at 0.78 μm, described by the asymmetry parameter $g = <cos(\theta_S)> = 0.38$, where θ_S is the scattering angle. This compares with g=0 for Rayleigh scattering, which has the phase function $P(\theta_S) = 3\ (1 + cos^2(\theta_S))/16\pi$, where $P(\theta_S)$ is the scattering probability per unit solid angle.

Prather (1974) and Sromovsky (2005) have shown that increasing the single scattering albedo has a highly non-linear effect on the total flux reflected by a planet at the full moon phase (defined here as ϕ=0°). The reflected flux (polarised flux plus unpolarised flux) at this phase is described by the geometric albedo, A_G, which is equal to unity for a flat isotropically scattering disc (a Lambert disc). For a pure Rayleigh scattering atmosphere A_G=0.80, whereas for our Rayleigh-like model with ϖ=0.99 the expected value declines to A_G=0.64 (Prather 1974). This is because a significant fraction of photons incident upon the planet require a large number of scattering events to escape the atmosphere. When ϖ<0.5, A_G is closer to a linear function of single scattering albedo, but at larger values of ϖ multiple scattering causes A_G to increase rapidly.

Although multiple scattering can greatly increase the geometric albedo, it also has a depolarising effect. This is because multiply scattered photons usually have lower polarisations than singly scattered photons, and the plane of polarisation typically differs also.

In order to determine how to relate our polarisation measurements to geometric albedos we have investigated the dependence of the polarisation on ϖ and the orientation of the orbit in space. To derive meaningful upper limits from the data in §3 we must consider not the absolute value of $P=\sqrt{(Q^2+U^2)}/I$ but the expected changes in Q/I and U/I during an orbital period, and the average of these over the range of possible orbital inclinations and orientations of the orbit projected in the plane of the sky.

We define the quantity $<\Delta QU>$ as the peak to trough polarisation modulation that we would typically expect to observe in at least one of Stokes Q/I or U/I for a planet with a Rayleigh scattering phase function and angular dependence of polarisation, after averaging over the ensemble of possible orbital inclinations and orientations in proportion to their probability (Prob(i)∝$sin(i)$). The maximum value of P during an orbit, denoted P_{MV}, is almost independent of orbital inclination, as shown by Seager et al.(2000). P_{MV} increases very slightly with decreasing orbital inclination, e.g. it is 7% higher at i=29° ($cos(i)$ = 0.9) than at i=87° ($cos(i)$=0.05). At large inclinations ($cos(i) \leqslant 0.25$) the polarisation lies mainly in one plane (see Figure 6(a-c)) and has a maximum of $P_{MV} \approx 1.2\times10^{-6}(\varpi/0.2)(r/0.05AU)^{-2}(R/1.2R_{Jup})^2$, for small values of ϖ, where r is orbital radius and R is the planetary radius. This would be detected as a maximum positive or negative excursion in Q/I or U/I from the small constant interstellar polarisation, which would occur near ϕ=±60°. Considering the range of possible orientations of the orbital as projected in the plane of sky, either Q/I and/or

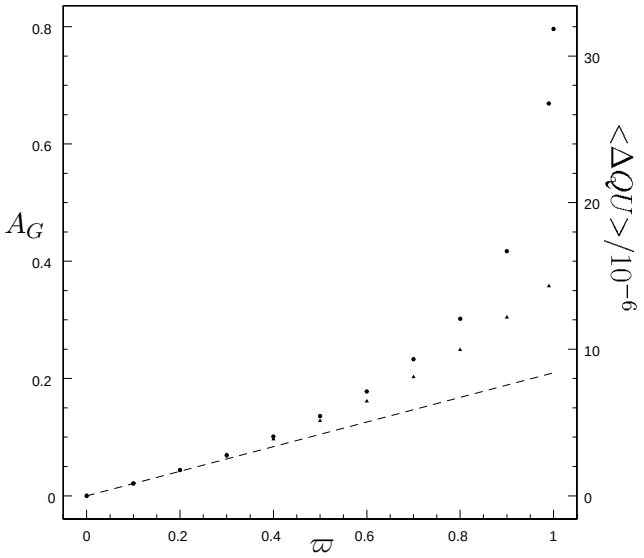

Figure 9. Geometric albedo, A_G and expected peak to trough polarisation modulation, $<\Delta QU>$, for a Rayleigh scattering atmosphere as a function of single scattering albedo, ϖ. The upper points (circles) represent A_G, shown on the left axis. The lower points (triangles) represent $<\Delta QU>$, shown on the right axis.

Table 6. Predicted geometric albedo, A_G, and expected polarisation properties as a function of single scattering albedo for planets with Rayleigh-like atmospheres (see text). The polarisation properties are calculated for a planet with R=1.2 R_{Jup} and r=0.05 AU and are given in units of 10^{-6}.

ϖ	A_G	$<\Delta QU>/10^{-6}$	$<P_{MV}>/10^{-6}$
1.0	0.796[a]	-	-
0.99	0.669	14.30	10.10
0.9	0.417	12.17	8.40
0.8	0.302	9.95	6.95
0.7	0.233	8.10	5.63
0.6	0.178	6.45	4.55
0.5	0.136	5.12	3.57
0.4	0.101	3.87	2.69
0.3	0.069	2.79	1.93
0.2	0.044	1.75	1.22
0.1	0.021	0.84	0.59

Note: (a) The geometric albedo of 0.796 for a pure Rayleigh scattering atmosphere with ϖ=1.0 is taken from Prather (1974).

U/I would have a variation of at least $P_{MV}/\sqrt{2}$, each having a statistical average of 0.9 P_{MV}. At smaller inclinations (see Figures 7 and 8) we see larger variations: both Q/I and U/I have variations $\gtrsim$ 1.5 P_{MV} over the course of an orbit as they change periodically from positive to negative in sign. For inclinations $cos(i) \geqslant 0.25$ we take the average of the full variations in Q/I, U/I and in the intermediate polarisation planes at position angles of 22.5° and 67.5° to predict the amount that would be observed. The magnitude of the variations in all these possible planes of polariation is similar. In the limiting case of i=0 we would expect that P is constant, while Q/I and U/I have equal amplitude, since the planet would always show a half moon phase in this 'pole-on' view of the orbit.

Averaging over the full range of inclinations, (weighting by their probability), we find that the typical peak to trough variation that we would expect to observe is $< \Delta QU > \approx 1.75\times10^{-6}(\varpi/0.2)(r/0.05AU)^{-2}(R/1.2R_{Jup})^2$, for small values of ϖ. Since the orbital inclination has only a modest effect on the sensitivity of polarisation measurements to extrasolar planets (when searching for periodic variations in the Stokes parameters) it is acceptable to use this value when placing limits on planets whose orbital inclination. is unknown.

In Table 6 and Figure 9 we show how $<\Delta QU>$, A_G and $<P_{MV}>$ change as functions of ϖ, for a planet at r=0.05 AU with radius R=1.2R_{Jup}. ($<P_{MV}>$ is the value of P_{MV} obtained after averaging over the range of orbital inclinations, i.e. it is the typical maximum polarisation of the planetary system that we would expect to observe in the course of an orbit, in the absence of polarisation due to the interstellar medium.) All these variables are close to linear functions of ϖ when ϖ is small, but increase more rapidly as ϖ approaches unity owing to the growing contribution of multiply scattered photons to the reflected flux. We find that $<\Delta QU>$ and $<P_{MV}>$ are closer than A_G to being linear functions of ϖ, owing to the depolarising effect of multiple scattering at high values of ϖ, which partly counterbalances the increased reflected flux. $<\Delta QU>$ and $<P_{MV}>$ have essentially identical dependences on ϖ and obey the simple relation $<\Delta QU>=1.43<P_{MV}>$ to within the ∼1% uncertainty imposed by the these Monte Carlo simulations with 2×10^7 photons. Wood et al.(1996) found a qualitatively similar dependence of polarisation on ϖ when modelling the scattering of light in a geometrically thin circumstellar accretion disc. The behaviour held true for all inclination angles of the disc.

The relation between $<\Delta QU>$ (the typical peak to trough polarisation modulation) and A_G is almost linear for $\varpi \leqslant 0.7$. The data in Table 6 show that the relation $<\Delta QU>=3.9\times10^{-5}A_G$ is valid to within ∼10% for $\varpi<0.7$, or $A_G<0.22$. For the more general case where R and r may be different and scattering may be only Rayleigh-like rather than Rayleigh (see §4.1), this becomes

$$(1) \quad <\Delta QU>=3.9\times10^{-5}p_m A_G(r/0.05AU)^{-2}(R/1.2R_{Jup})^2$$

Table 6 shows that when ϖ=0.99, $P_{MV}\approx1.0\times10^{-5}$ for a planet at r=0.05 AU with R=1.2R_{Jup}. For a transiting planet such as HD189733 b with $i\approx90°$ the peak to trough variation in Q/I and U/I would typically be 0.9 P_{MV}, as noted earlier, and the maximum possible value would be P_{MV}. HD189733 b has r=0.031 AU and R=1.2 R_{Jup} (Miller-Ricci et al.2008; Winn et al.2007; Pont et al.2007; Baines et al.2007) so when we scale to the smaller orbital radius we find that the expected peak to trough variation would typically be 2.3×10^{-5}, with a maximum possible value of 2.6×10^{-5} for this Rayleigh scattering model with ϖ=0.99. It is therefore hard to see how to explain the variations in Q/I and U/I at a level $\geqslant10^{-4}$ that were reported by Berdyugina et al.(2008).

4.3 Upper limits on the planets around 55 Cnc and τ Boo

The inclination and orientation of the projected orbits of the planets around 55 Cnc is not known with high precision or confidence so we cannot predict whether a variation should more easily be seen in Q/I or U/I. The inclination given in Table 1 is only an estimate. By contrast, the inclination of the orbit of τ Boo b is constrained to be $i\sim40°$ with fair confidence (see §1).

Inspection of Figures 2 and 3 shows that the datasets have far from complete phase coverage. Nonetheless, the datasets for both 55 Cnc e and τ Boo b are sensitive to the full variations in Stokes Q/I and/or U/I predicted for all possible inclinations. For 55 Cnc b, which has a longer orbital period (see Table 1), the range of orbital angles covered by the data is 206° to 334°. This range of angles samples between 67% and 100% of the predicted peak to trough variation in at least one of Q/I and U/I, depending on the orbital inclination. The average value is approximately 75% and we use this value to derive the upper limit for that planet.

No variations of the nightly averages are detected that are consistent with those that might be expected from Figures 6, 7 and 8. Figure 7(a-c) illustrates the likely form of the variations for τ Boo. However, it should be noted that the orientation of the axis of the projected orbit in the plane of the sky need not lie parallel to the Stokes Q or U planes. If it lies at a position angle of 22.5° (compared to 0° for Q and 45° for U) then the expected signal has the form of the average of the Q/I and U/I curves, multiplied by $\sqrt{2}$.

We use the standard deviation of the nightly averages to determine an upper limit on the polarisation variations in both planets, including only nights with at least two data points. The standard deviations of the Q/I and U/I nightly averages for 55 Cnc are $\sigma_{n-1} = 2.16\times10^{-6}$ and $\sigma_{n-1} = 2.31\times10^{-6}$ respectively. Taking the average of these gives us a standard deviation of 2.24×10^{-6}. For the hot Neptune 55 Cnc e this corresponds to a 4σ sensitivity limit of $A_G<0.13(R/1.2R_{Jup})^{-2}p_m^{-1}$, using eq.(1) from §4.2, which is valid for planets with low albedos. If we assume a somewhat smaller radius, e.g. 0.8R_{Jup}, for 55 Cnc e then the 4σ upper limit corresponds to a larger single scattering albedo and the formula is no longer valid. E.g. for the case R=0.8R_{Jup} the 4σ limit is $A_G \lesssim 0.38p_m^{-1}$. If the radius is even smaller then the data no longer place strong limits on A_G.

For the hot Jupiter 55 Cnc b the data do not provide a useful upper limit. For a highly reflective planet at r=0.05 AU with ϖ=0.99, Table 6 indicates that $<\Delta QU>=1.43\times10^{-5}$. After scaling this to the actual orbital radius of 0.115 AU and correcting for the 75% factor caused by the limited phase coverage, the expected peak to

trough polarisation variation is only $< \Delta QU >=2.0\times10^{-6}$, which is slightly less than the 1σ sensitivity of the data.

For τ Boo the standard deviations of the Q/I and U/I nightly averages are $\sigma_{n-1} = 3.62 \times 10^{-6}$ and $\sigma_{n-1} = 6.49\times10^{-6}$ respectively. Taking the average of these gives us a standard deviation of 5.06×10^{-6}. Assuming that the orbital inclination is $i\sim40^\circ$, the expected peak to trough variation in the Q/I and U/I parameters is $5.1\times10^{-5}A_G$ (taking the average of the variations in Q/I, U/I and the polarisation planes at 22.5° and 67.5°). This leads to a 4σ sensitivity limit of $A_G<0.37(R/1.2R_{Jup})^{-2}p_m^{-1}$. We note that the smaller standard deviations for subset of data taken in 2005 for this planet could in principle be used to establish a more sensitive limit. However, the phase coverage in the 2005 data is not fully sensitive to the predicted polarisation variations so we adopt the larger standard deviations associated with the full dataset.

The upper limit for τ Boo b is similar to those previously reported at shorter visible wavelengths by Charbonneau et al.(1999) and Leigh et al.(2003), based on searches for Doppler shifts in stellar absorption lines after reflection by the planet.

These datasets therefore provide useful upper limits on the reflected light from 55 Cnc e and τ Boo b but not for 55 Cnc b, which has a larger orbit. It is notable that the data for τ Boo are more than a factor of two less stable than the data for 55 Cnc, even though the τ Boo data points have 42% smaller uncertainties due the smaller photon noise for the brighter star. The scatter in the 55 Cnc data is consistent with the internal errors, whereas the scatter in the τ Boo data is not, see §3.2.

4.4 Stability of interstellar polarisation

The relatively large dataset on bright nearby stars taken in February 2006 provides some redundancy in the fit to telescope polarisation. Assuming the sample of five stars in Table 3 is representative, we can infer that nearby stars with a wide range of spectral types have no variations from night to night above a typical 1σ level of $\sim 2\times10^{-6}$. In calculating this figure we have excluded from the nightly averages ten outlying measurements (13% of the data) that depart from the TP fit by $>3\sigma$ and $>3\times10^{-6}$, see §2.3

In addition, three of the nearby bright stars have repeat observations separated by a year or more. HR4540 was observed in 2004, 2005 and 2006. HR5854 was observed in 2004 and 2005 and HR4534 was observed in 2005 and 2006. HR4540 shows no variation between the three epochs within 1σ uncertainties of $\approx2.2\times10^{-6}$. HR5854 shows differences between 2004 and 2005 of $5.2\pm2.0\times10^{-6}$ in Q/I and $5.1\pm2.2\times10^{-6}$ in U/I. HR4534 shows differences of between 2005 and 2006 of $3.2\pm1.7\times10^{-6}$ in Q/I and $-8.1\pm1.5\times10^{-6}$ in U/I. Most of these apparent differences have $<3\sigma$ significance so we cannot say with certainty whether real variations in the polarisation have been detected with such a small sample of measurements. We note that the apparently significant change in the U/I measurement for HR4534 would appear smaller and have a larger uncertainty if we had not excluded two outlying readings from the average 2006 measurement given in Table 2.

It is therefore unclear whether the polarisation of nearby stars is stable enough on timescales of years to define very low polarisation standards for general use by the community. If this were possible it would allow high precision polarimeters to be used at equatorially mounted telescopes (for which the TP cannot be separated from the polarisation of the light source) and allow them to be used at telescopes with alt-azimuth mounts without the need for such lengthy calibration observations.

The apparent stability of the polarisation measurements within each observing run suggests that neither normal stars nor the interstellar medium in the local ionised bubble produce variable polarisation on timescales of a few days and that at most only modest changes occur on timescales of years. The typical relative stellar motions of 10 kms^{-1} in the solar neighbourhood cause the dust column sampled by the line of sight through the interstellar medium to change on a timescale of a few days for nearby stars. Assuming that the observed polarisations are due to dichroic extinction by interstellar dust grains aligned with the local magnetic field, we can therefore conclude the dust density, degree of aligment and magnetic field direction is typically uniform on spatial scales up to 6×10^9m (corresponding to the movement of the dust column in a week) and that large changes do not occur on scales up to $\sim$1 AU (corresponding to the motion in a year).

4.5 New detectors

PLANETPOL employs Avalanche Photodiode Detectors (APDs) to detect the incident radiation. Subsequent to the observations reported in this paper, it was found (during brief observations with the same telescope in November 2006) that the S2383 APDs used for these observations and in Hough et al.(2006) (detector size 1mm, gain 100) can be usefully replaced by S2384 APDs (detector size 3mm, gain 50) for stars brighter than I $\sim$ 8.5 mag., using a 4-m class telescope with no filter. Although the intrinsic noise of the S2384 APD is $\sim$ 7.5 times that of the S2383, the excess noise produced by the avalanche process, which is poportional to the photon noise, is somewhat lower. The overall signal to noise ratio, as measured by the internal errors on individual measurements, is improved by 40% for bright stars. This is equivalent to a factor of two in observing speed. This reduces the photon noise multiplicative factor of $\sim$2.5 reported by Hough et al.(2006) to $\sim$1.8. The two detector assemblies can easily be interchanged as the Fabry lenses, different for the two APDs, are an integral part of these assemblies.

5 CONCLUSIONS

The strong upper limit for 55 Cnc e, $A_G<0.13(R/1.2R_{Jup})^{-2}p_m^{-1}$, is hard to explain in terms of a low albedo. At the time the observations were planned there were no available calculations or data concerning the likely size of very strongly irradiated Neptune mass planets. Subsequent calculations by Baraffe et al.(2006) suggest that while a wide range of sizes (0.4 R_{Jup} to $\sim$ 1 R_{Jup} are possible, it is likely that hot Neptune planets will usually have radii $\leqslant 0.6R_{Jup}$. The larger radii can occur for hydrogen and helium dominated Neptune mass planets but these may evaporate on a relatively short timescale. Unfortunately the physics of the evaporation process is

still not clearly established. The sole known transiting hot Neptune, GJ436b, has a radius between 0.38 and 0.44 R_{Jup} (Gillon et al.2007a; 2007b; Deming et al.2007; Bean et al.2008; Torres et al.2007), though this may not be a useful comparison planet owing to the much weaker irradiation from its M2V star. Our non-detection of 55 Cne e is most easily explained by a relatively small planet. The data allow us to rule out a Jupiter sized planet with even a low geometric albedo and also rule out a 0.8 R_{Jup} planet with a moderate albedo. However, we caution that it is possible for planets to have very low geometric albedos. For example the radiative transfer could be dominated by very small dust particles with a very small single scattering albedo. Also, if there is no high altitude dust layer, strong atomic and molecular absorption features such as the KI resonant line at 770 nm could reduce the geometric albedo in the PLANETPOL passband. Furthermore, Hood et al.(2008) have shown that 3D structure in planetary atmospheres can reduces the geometric albedo by a large fraction, relative to homogeneous atmospheres such as those modelled in this work. Hence a planetary radius as high as R=1.2 R_{Jup} cannot be entirely ruled out.

We conclude from the upper limit for τ Boo b that this is a fairly dark planet in our 590-920 nm passband. This extends the similar limits that were found by Charbonneau et al.(1999) and Leigh et al.(2003) at shorter wavelengths by searching for Doppler shifted absorption lines in the stellar spectrum. A non-detection at an upper limit of A_G<0.37$(R/1.2R_{Jup})^{-2}p_m^{-1}$ is not particularly surprising in view of the possible absorption mechanisms described above. The most plausible example model of Seager et al.(2000), in which the scattering is dominated by a mixture of three types of 0.1 μm grains, gave A_G = 0.175. Nonetheless, the data indicate that τ Boo b is less reflective than Jupiter and Saturn, which have A_G≈0.5 throughout most of the PLANETPOL passband (Karkoschka et al.1994). This is of course subject to the assumption that the scattering particles have Rayleigh-like polarisation behaviour, i.e. the scattering is dominated by molecules or by dust particles $\lesssim$0.1 μm in radius. Both our data and the *MOST* data indicate that this planet is not an ideal target for the highest precision studies.

Our multiple scattering model atmosphere calculations indicate that the large amplitude periodic polarisation signal from the HD189733 system that was reported by Berdyugina et al.(2008) cannot be explained in terms of reflected light from the planet HD189733b. If the observations are confirmed it would be important to consider the possible contribution of star spots to the polarisation of the system, given that HD189733 is an active star with much larger photometric variations than τ Boo or 55 Cnc, e.g. Winn et al.(2007).

The measurements for nearby stars with low polarisation are stable on timescales of a week. It is not yet clear whether they are stable at the 10^{-6} level on timescales of a year. Finally, we note that these results do not represent the full potential of the instrument. The new detectors offer a 40% improvement in sensitivity, so observations of stable bright hot Jupiter systems such as υ And and 51 Peg would offer a good chance of a successful detection. The new class of very hot Jupiters recently detected by transit surveys around fainter stars may also offer good prospects for observation. Transiting planets, which have i≈90°, display the full range of phase angles (0-180°) during the course of an orbit, thereby offering the maximum possible amount of information. For the purpose of simple detection, there is less need to sample the full phase curve since the most likely timing of maximum polarisation is predictable if we know that i≈90° and assume that the scattering phase function is not highly aniostropic. However, the expected amplitude of the periodic polarisation changes in Stokes Q/I and U/I is slightly smaller at i=90° than for smaller inclinations, and we caution that planets in such small orbits might induce variable polarisation on their central star due to star spots.

6 ACKNOWLEDGMENTS

We wish to thank the staff of the William Herschel Telescope and the members of the PPARC grant panel who supported this project. PLANETPOL was partially funded by a 100k grant from PPARC, the predecessor to the UK Science and Technology Facilties Council. We also thank Matt Giguere, Debra Fischer and Geoff Marcy for providing orbital phase information for 55 Cnc e and τ Boo b.

REFERENCES

Ackerman A.S., Marley M.S., 2001, ApJ, 556, 872
Bailey J., Ulanowski Z., Lucas P.W., Hough J.H., Hirst E., Tamura M., 2008, MNRAS 386, 1016
Baines E.K., van Belle G.T., ten Brummelaar T.A., McAlister H.A., Swain M., Turner N.H., Sturmann L., Sturmann J., 2007, ApJ, 661, L195
Bakos G., Noyes R.W., Kovács G., Stanek K.Z., Sasselov D.D., Domsa I., 2004, PASP, 116, 266
Baliunas S.L., Solokoff D., Soon W., 1996, ApJ, 457, L99
Baliunas S.L., Henry G.W., Donahue R.A., Fekel F.C., Soon W.H., 1997, ApJ, 474, L119
Baraffe I., Alibert Y., Chabrier G., Benz W. 2006, A&A 450, 1221
Bean J.L., Benedict G.F., Charbonneau D., Homeier D., Taylor D.C., McArthur B., Seifahrt A., Dreizler S., Reiners A., 2008, A&A in press, astro-ph/0806.0851
Berdyugina et al.2008, ApJ, 673, L83
Borra E.F., Vaughn a.H., 1976, ApJ, 210, L145
Butler R.P., Marcy G.W., Williams E., Hauser H., Shirts P., 1997, ApJ, 474, L115
Butler R.P., Wright J.T., Marcy G.W., Fischer D.A., Vogt S.S., Tinney C.G., Jones H.R.A., Carter B.D., Johnson J.A., McCarthy C., Penny A.J., 2006, ApJ, 646, 505
Burrows A., Hubeny I., Budaj J., Knutson H.A., Charbonneau D..2007, ApJ, 668, L171
Carciofi A.C., Magalhães A.M., 2005, ApJ, 635, 570
Catala C., Donati J.-F., Shkolnik E., Bohlender D., Alecian E., 2007, MNRAS, 374, L42
Charbonneau D., Noyes R.W., Korzennik S.G., Nisenson P., SaurabhJ., Vogt S.S., Kibrick R.I., 1999, ApJ, 522, L145
Charbonneau D., Brown T.M., Noyes R.W., Gilliland R.L.2002, ApJ, 568, 377
Claret A., 2000, A&A, 363, 1081
Deming D., Harrington J., Laughlin G., Seager S.,

Navarro S.B., Bowman W.C., Horning K., 2007, ApJ, 667, L199
Eggenberger A., Udry S., Mayor M., 2004, A&A, 417, 353
Fischer O., Henning Th., & Yorke H.W., 1994, A&A, 284, 187
Fischer D., Marcy G., Butler P., Vogt S., Laughlin G., Henry G., Abouav D., Peek K., Wright J., Johnson J., McCarthy C. & Isaacson H., 2008, ApJ, 675, 790
Gillon M., Pont F., Demory B.-O., Mallmann F., Mayor M., Mazeh T., Queloz D., Shporer A., Udry S., Vuissoz C., 2007, A&A, 472, L13 (2007a)
Gillon M., Demory B.-O., Barman T., Bonfils X., Mazeh T., Pont F., Udry S., Mayor M., Queloz D. 2007, A&A, 471, L51 (2007b)
Green D., Matthews J., Seager S., Kuschnig R., 2003, ApJ, 597, 590
Hansen J.E., Hovenier J.W., 1974, J. Atmos. Sci., 31, 1137
Harrington J., Hansen B.M., Luszcz S.H., Seager S., Deming D., Menou K., Cho J.Y.-K., Richardson L.J., 2006, Science, 314, 623
Helling Ch., Woitke P., & Thi W.F., 2008, A&A, 485, 547
Hood B., Wood K., Seager S., Collier Cameron A., 2008, MNRAS, 389, 257
Hough J.H., Lucas P.W., Bailey J.A., Tamura M., Hirst E., Harrison D., Bartholomew-Biggs M. 2006, PASP, 118, 1302
Karkoschka E., 1994, Icarus, 111, 174
Kemp J.C., Wolstencroft R.D., 1973, ApJ 179, L33
Kemp J.C., Henson G.D.,Steiner C.T., Powell E.R., 1987, Nature, 326, 270
Knutson H.A., Charbonneau D., Allen L.E., Fortney J.J. et al.2007, Nature, 447, 183
Knutson H.A., Charbonneau D., Allen L.E., Burrows A., Megeath S.T., 2008, ApJ, 673, 526
Lecavelier des Etangs, Pont, Vidal-Madjar, Sing, 2008, A&A, 481, L83
Leigh C., Collier Cameron A., Horne K., Penny A., James D., 2003, MNRAS 344, 1271
Leroy J.-L., 2000, 'Polarization of light and astronomical observation', pub. Gordon & Beach, Amsterdam
McArthur B.E., Endl M., Cochran W.D., Benedict G.F., Fischer D.A., Marcy G.W., Butler R.P., Naef D., Mayor M., Queloz D., Udry S., Harrison T.E., 2004, ApJ, 614, L81
Marcy G.W. Butler R.P., Fischer D.A., Laughlin G., Vogt S.S., Henry G.W., Pourbaix D. 2002, ApJ, 581, 1375
Mayor M., Queloz D., 1995, Nature, 378, 355
Miller-Ricci E., Rowe J.F., Sasselov D., Matthews J.M., Kuschnig R., Croll B., Guenther D.B., Moffat A.F.J., Rucinski S.M., Walker G.A.H., Weiss W.W., 2008, ApJ, 682, 593
Patience J., White R.J., Ghez A.M., McCabe C., McLean I.S., Larkin J.E., Prato L., Kim S.S., Lloyd J.P., Liu M.C, Graham J.R., Macintosh B.A., Gavel D.T., Max C.E., Bauman B.J., Olivier S.S., Wizinowich P., Acton D.S., 2002, ApJ, 581, 654
Pollacco D.L., Skillen I., Collier Cameron A., Christian D.J., Hellier C., Irwin J., Lister T.A., Street R.A., West R.G., et al. 2006, PASP, 118, 1407
Pont F., Gilliland R.L., Moutou C., Charbonneau D., Bouchy F., Brown T.M., Mayor M., Queloz D., Santos N., Udry S., 2007, A&A, 476, 1347
Pont F., Knutson H., Gilliland R.L., Moutou C., Charbonneau D., 2008, MNRAS, 385, 109
Prather M.J., 1974, ApJ, 192, 787
Raghavan D., Henry T.J., Mason B.D., Subasavage J.P., Jao, W.-C., Beaulieu T.D., & Hambly N.C., 2006, ApJ, 646, 523
Rowe, Matthews, Seager, Kuschnig et al., 2007, 0711.4111
Schneider J., 2008, on-line: http://exoplanet.eu/
Seager S., Whitney B.A., Sasselov D.D., 2000, ApJ 540, 504
Serkowski K., 1974, in "Planets, Stars and Nebulae studies with Photopolarimetry", p135, ed. T.Gehrels, University of Arizona Press, Tucson, USA.
Shkolnik E., Walker G.A.H., Bohlender D.A., Gu P.-G., Kurster M., 2005, ApJ, 622, 1075
Snellen I.A.G., 2005, MNRAS, 363, 211
Snellen I.A.G., Covino E., 2007, MNRAS, 375, 307
Soderblom D.R., 1985, AJ, 90, 2103
Sromovsky L.A., 2005, Icarus, 173, 284
Stam D.M., Hovenier J.W., Waters L.B.F.M., 2004, A&A, 428, 663
Stam D.M., De Rooij W.A., Cornet G., Hovenier J.W., 2006, A&A, 452, 669
Stam D.M., 2008, A&A, 482, 989
Swain M.R., Vasisht G., Tinetti G., 2008, Nature 452, 329
Tinetti G., Vidal-Madjar A., Liang M-C., Beaulieu J-P., Yung Y., Carey S., Barber R.J., Tennyson J., Ribas I., Allard N., Gilda E.B., Sing D.K., Selsis F., 2007, Nature, 448, 169
Torres G., 2007, ApJ 671, L65
Ulanowski Z., Bailey J., Lucas P.W., Hough J.H., Hirst E., 2007, Atm. Chem. & Phys., 24, 6161
Walker G.A.H., Croll B., Matthews J.M., Kuschnig R., Huber D., Weiss W.W., Shkolnik E., Rucinski S.M., Guenther D.B., Moffat A.F.J., Sasselov D., 2008, A&A, 482, 691
Winn J.N., Holman M.J., Henry G.W., Roussanova A., Enya K., Yoshii Y., Shporer A., Mazeh T., Johnson J.A., Narita N., Suto Y., 2007, AJ, 133, 1828
Winn J.N., Holman M.J., Shporer A.. Fernández, José, Mazeh T., Latham D.W., Charbonneau D., Everett M.E., 2008, AJ, 136, 267
Wood K., Bjorkman J.E., Whitney B., Code A., 1996, ApJ 461, 847